Environment Canada

Water Science and Technology Directorate

Direction générale des sciences et de la technologie, eau

Environnement Canada

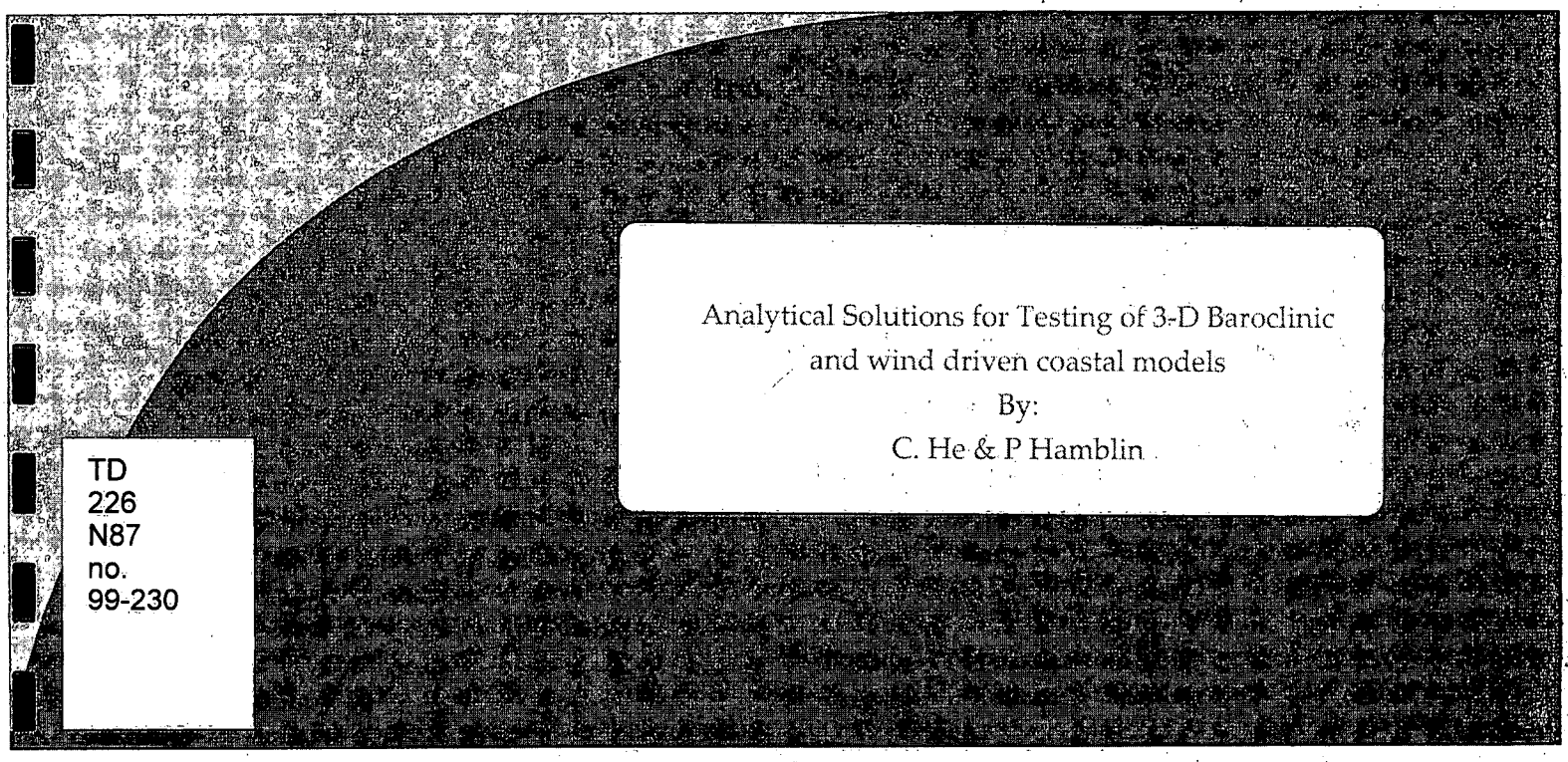

Analytical Solutions for Testing of 3-D Baroclinic and wind driven coastal models

By:

C. He & P Hamblin

MANAGEMENT PERSPECTIVE

Title:	**Analytical Solutions for testing of 3-D baroclinic and wind driven coastal models.**
Author(s):	*C.He and* ***P.Hamblin****, AERB .*
NWRI Publication #:	99-230
Citation:	*To be published as a contribution to modelling in the coastal zone.*
EC Priority/Issue:	*In response to a proposal to divert treated sewage from Hamilton Harbour to Lake Ontario a model development was undertaken. This is the first reporting on the model development in an international journal .*
Current Status:	*This document reports on the temperature and flows suitable for testing three-dimensional mathematical models in lakes and coastal zones.*
Next Steps:	*These results will be disseminated to the appropriate persons making the decisions on how best to manage the coastal zone on Lake Ontario.*

Analytical Solutions for Testing of 3-D Baroclinic and Wind Driven Coastal Models

Cheng He and Paul F. Hamblin
Aquatic Ecosystem Restoration Branch, National Water Research Institute, Burlington, Ontario, CANADA
cheng.he@cciw.ca
paul.hamblin@cciw.ca

Abstract
It is always challenge for a model developer to verify three dimensional hydrodynamic and transport models, especially for the baroclinic term over variable topography, due to a lack of observational data sets or the availability of suitable analytical solutions. Heat flux through the water surface and wind stress are the two main forces controlling the stratification of a water body. In this paper, exact solutions for periodic forcing by surface heat flux and wind stress, are given by solving the linearized equations of motion in a three dimensional domain neglecting the rotational and horizontal diffusion terms. The temperature at the bottom is set to a prescribed periodic value and a linear slip condition on flow is enforced at the bottom. The geometry of the quarter annular, which has been extensively studied for 2-D and 3-D analytical solutions of unstratified water bodies, with a general power law variation of bottom slope in the radial direction and constant in the azimuthal direction is used. The analytical solutions are derived in a cylindrical coordinate system, which describes the 3-D fluid field in a Cartesian coordinate system. The results presented in this paper should provide a foundation for the study the treatment of the baroclinic term over topography in 3-D numerical models.

Introduction

Various numerical methods for the solution of the Navier-Stokes equations have been applied to problems of flood routing, tidal circulation, storm surges and contaminant transport in coastal areas. The utility of such methods is often demonstrated by comparison of the computed variables with field observations. However, this type of comparison is often incapable of adequately verifying that numerical model accurately represents the dynamics of the study region, for example, Hackett and Roed (1994). The limitations of this approach are due to incomplete understanding of the behavior of the numerical procedure and inadequate data. Observations of three dimensional components of flow are rarely available throughout the temporal and spatial domains of interest. Thus, in general, data bases are inadequate tools for establishing that a numerical model is correctly solving the governing equations. This is particularly true for vertical velocity which is too small to measure but is of practical importance to such phenomena as coastal upwelling.

The precision with which a numerical scheme solves the full governing equations should also be established. Because of the nonlinearities in the equations, this is difficult to ascertain precisely. Furthermore the effect of an irregularly shaped boundary on the accuracy of the numerical solution is generally not completely known although it is acknowledged to be important.

Lacking suitable analytical solutions for testing the output of three-dimensional numerical models various authors (Tartinville et al. 1998 and Beletsky et al. 1997) have resorted to comparing various models with one another. The difficulty with this approach is that it is hard to determine which model is correct.

These various sources of error and uncertainty in verification can sometimes be obscurred in the numerical solution by adjustment of such parameters as bathymetry, the eddy coefficients, and the bottom drag coefficients. It is our belief that a more systematic and rigorous assessment of error sources must be made in order to establish the credibility of a numerical model. To this end a number of analytical solutions are herein developed which should prove useful for comparison with numerical solutions. By necessity, the governing equations have been linearized. However, heat flux through water surface, bottom and internal friction, wind stress, and variable bathymetry have been incorporated into the equations. Solution for the dynamic steady state with a periodic forcing function is obtained. In line with the philosophy that these solutions are useful primarily as tools for model verification rather than solutions to actual field problems, emphasis is placed on periodic solutions.

A number of modellers have developed analytical solutions to aid in the development of their models. These may be classified into open with an offshore boundary condition and closed basin solutions with no flux boundary conditions. By far the most widely used analytical solutions for the purposes of verification of coastal numerical models are the solutions for quarter annular geometry. This geometry is particular useful as a test of a model's ability to treat curved boundaries. The analytical solution for the depth-averaged case was developed by Lynch and Gray (1978) for constant, linear, and quadratic bathymetry for both steady state wind setup and periodic tidal response. Their analytic solution was extended to three dimensions and rotation by Lynch and Officer(1985). Lynch and Werner (1987) calculated and displayed this analytical solution for tidal oscillations near a circular island where the tidal amplitude at the open ocean boundary varies with position. Muccino et al.(1997) who recognized the importance of vertical velocity gave an

expression for the vertical velocity associated with the Lynch and Officer case but with a spatially constant tidal amplitude forcing at the open boundary. Hannah and Wright (1995) tested a three-dimensional finite element model with an analytical solution for linear depth-dependent wind-driven flows along a rotating coastline. All of these analytical solutions deal with unstratified water bodies. Once stratification over variable bathymetry is added, numerical models employing vertically stretched co-ordinates have difficulty resolving the baroclinic terms (Hanney,1991) so that analytical solutions are needed in the stratified case as well.

By prescribing the density field, Loder(1980) introduced exact solutions for U(x,z) and V(x,z) under the condition of zero depth-integrated cross-front transport and vertically uniform viscosity. Farrow and Patterson (1993 and 1994) developed analytical solutions for two thermally driven flows for a two-dimensional linearly sloping bottom neglecting advection but allowing for vertical diffusion. In closed basins a number of modellers have exploited the wind-driven flat bottomed analytical solutions of Csanandy (1968). However, Mass and Lam (1995) presented some free modes of oscillation over variable topography, uniform rate of stratification, no friction or diffusion but linearized advection in a two-dimensional closed basin. Their solutions are interesting as there is a two-way coupling between the mass and velocity fields through advection unlike the solutions of Farell and Patterson (1993 and 1994) and Fortatuno and Baptista (1996) where the density field is prescribed. As forcing and friction are neglected in the solutions of Mass and Lam (1995) it is not clear how they can be used in coastal model validation.

In this paper we develop analytical solutions aimed at verifying three dimensional hydrodynamic models, especially for improving numerical schemes for calculating the baroclinic terms. We start with solving the vertical temperature diffusion equation in a quarter annulus which leads to a variable density field which, in turn, drives the circulation. Wind forcing is also included. For simplicity, advection, horizontal diffusion and rotation terms are neglected. The vertical velocity is computed from the continuity equation. The rigid lid surface boundary condition is also assumed. A general power law dependence of depth with offshore distance allows for testing of numerical schemes for various degrees of bottom slope.

Analytical Solution In σ-Coordinate System

The similar quarter annular bathymetry and radial coordinate system as used by Lynch and Officer (1985) will be adopted in this study which is shown in plan in Fig. (1a) and in section in Fig. (1b). Because the governing equations, boundary

conditions and domain geometry do not depend on the azimuthal direction, variation occurs only in the radial and vertical directions.

The stratification is generated by a periodic heat flux applied to the water surface. Here we seek periodic solutions of the form $f(r,z,t) = \mathrm{Re}[f_0(r,z)e^{i\omega t}]$ for temperature and velocities. The governing equation of temperature in linearized and harmonic form with the horizontal diffusion and advection terms neglected is:

$$i\omega T_0 - D\frac{\partial^2 T_0}{\partial z^2} = 0 \qquad (1)$$

at surface

$$D\frac{\partial T_0}{\partial z} = hF_0 \qquad z = 0 \qquad (2)$$

and at bottom

$$T_0 = B_0 \qquad z = -h \qquad (3)$$

in which $T_0(z)$ is the complex amplitude of the temperature, $D = N_T h^2$ is the diffusivity of temperature, ω is the radian frequency, hF_0 is the amplitude of the heat flux at water surface, $h(r) = h_0 r^m$ (h_0 is a constant and m is unrestricted constant) is the bathymetric relation, r is the radial coordinate, and B_0 is the amplitude of the temperature specified at the bottom. The reciprocal of N_T may be interpreted as the thermal spin-up time.

By use of the σ-coordinate, the temporally and spatially varying water depth can be transformed into uniform depth, which can simplify the numerical formulation.

$$\sigma = \frac{z}{h} \qquad (4)$$

In a general σ-coordinate system (where σ=0 at the free surface and σ=-1 at the bottom), the governing equation and boundary conditions become:

$$\frac{\partial^2 T_0}{\partial \sigma^2} - \frac{i\omega}{N_T} T_0 = 0 \qquad (5)$$

$$N_T h^2 \frac{\partial T_0}{h\partial \sigma} = hF_0 \qquad \sigma = 0 \qquad (6)$$

$$T_0 = B_0 \qquad \sigma = -1 \qquad (7)$$

The solution of equation (5) with boundary conditions (6) and (7) is:

$$T_0 = M_1 \cosh(\zeta\sigma) - M_2 e^{-\zeta\sigma} \qquad (8)$$

with

$$M_1 = \frac{1}{\cosh\zeta}(B_0 + \frac{F_0}{N_T\zeta}e^{\zeta}) \tag{9}$$

$$M_2 = \frac{F_0}{N_T\zeta} \tag{10}$$

$$\zeta^2 = \frac{i\omega}{N_T} \tag{11}$$

Next, the density field can be calculated from the temperature solution. Here, we assume that density is linearly related to temperature as:

$$\rho = a_T T + b \tag{12}$$

where a_T is constant and b is a reference density, so the complex amplitude of the density difference, $\Delta\rho_0$, with respect to the reference density at any point is:

$$\Delta\rho_0 = a_T T_0 \tag{13}$$

The complex amplitude of baroclinic pressure, P_0, as a function of depth associated with the density variation is:

$$P_0 = \frac{g}{\rho_w} h \int_{\sigma}^{0} \Delta\rho_0 \, d\sigma$$

$$= \frac{g a_T}{\rho_w \zeta} h[M_2(1 - e^{-\zeta\sigma}) - M_1 \sinh(\zeta\sigma)] \tag{14}$$

where g is gravity and ρ_w is water reference density. The baroclinic term in the radial direction, then, can be computed in σ coordinates:

$$\frac{\partial P_0}{\partial r} = (\frac{\partial}{\partial r} - \frac{2\sigma}{r}\frac{\partial}{\partial\sigma})P_0$$

$$= \frac{a_T g h_0 r^{m-1}}{\rho_w \zeta}\{M_2[m - (m + 2\sigma\zeta)e^{-\zeta\sigma}] + M_1[2\sigma\zeta\cosh(\zeta\sigma) - m\sinh(\zeta\sigma)]\} \tag{15}$$

After the expression for the baroclinic term has been obtained, the 3-dimensional velocity field driven by baroclinic forcing and wind stress can be computed from the momentum equation. We assume that the free surface elevation is zero everywhere for all time (rigid lid free surface) and that wind stress has the same frequency as the heat flux through the free surface. The momentum equation without advection, rotation, free surface pressure and horizontal diffusion terms is:

$$\frac{\partial u}{\partial t} = -\frac{g}{\rho_w}\frac{\partial P}{\partial r} + D_v \frac{\partial^2 u}{\partial z^2} \tag{16}$$

where $D_v = N_v h^2$ is the vertical viscosity, and N_v is a constant. The horizontal velocity is decomposed by separation of variables with the form $u(r,z,t) = U_0(r,z)e^{i\omega t} = u_r(r)u_0(z)e^{i\omega t}$, where

$u_0(z)$ is the unknown complex amplitude of the horizontal velocity depending only on the vertical coordinate, z, and $u_r(r) = r^{m-1}$. By substituting u and the solution for baroclinic term (15), equation (16) becomes in the σ-coordinate system:

$$\frac{\partial^2 u_0}{\partial \sigma^2} - \frac{i\omega}{N_v} u_0 = \frac{a_T g h_0}{\rho w \zeta N_v} \{M_2[m-(m+2\sigma\zeta)e^{-\zeta\sigma}] + M_1[2\sigma\zeta\cosh(\zeta\sigma) - m\sinh(\zeta\sigma)]\} \quad (17)$$

with the boundary conditions,

$$N_v h^2 \frac{\partial u_0}{h\partial\sigma} = \tau_w h \qquad \sigma = 0 \quad (18)$$

and

$$N_v h^2 \frac{\partial u_0}{h\partial\sigma} = \tau_b h u_0 \qquad \sigma = -1 \quad (19)$$

where $h\tau_w$ is the wind stress and $h\tau_b$ is the bottom slip parameter. The general solution to equation (17) is:

$$u_0 = Ae^{\xi\sigma} + Be^{-\xi\sigma} + Q \quad (20)$$

where

$$\xi^2 = \frac{i\omega}{N_v} \quad (21)$$

and Q is the particular solution which has two forms depending on the Prandtl number ($\xi = \zeta$, $\Pr = 1$) and ($\xi \neq \zeta$, $\Pr \neq 1$). The details of the particular solutions are given in Appendix A.

In following, we concentrate on the solution for case $\xi \neq \zeta$ which represents more general applications. The result for the case $\xi = \zeta$ is given in Appendix B.

As an aid to understanding the steps followed in the solution procedure the expression for $\frac{\partial u_0}{\partial \sigma}$ is given here by differentiating (20) and from Q in Appendix A:

$$\frac{\partial u_0}{\partial \sigma} = \xi(Ae^{\xi\sigma} - Be^{-\xi\sigma}) + \frac{G}{\Pi}\{M_1\{[(2-m)\zeta - \frac{4\zeta^3}{\Pi}]\cosh(\zeta\sigma) + 2\zeta^2\sigma\sinh(\zeta\sigma)\}$$

$$- M_2[(2-m)\zeta - 2\sigma\zeta^2 - \frac{4\zeta^3}{\Pi}]e^{-\zeta\sigma}\} \quad (22)$$

where

$$\Pi = \zeta^2 - \xi^2 \quad (23)$$

$$G = \frac{g a_T h_0}{\rho_w \zeta N_v} \quad (24)$$

Substituting (22) into the boundary conditions (18) and (19) yields;

$$A\xi - B\xi + G\frac{(2-m)\zeta - \frac{4\zeta^3}{\Pi}}{\Pi}(M_1 - M_2) = \frac{\tau_w}{N_v} \qquad \sigma = 0 \tag{25}$$

$$A\xi e^{-\xi} - B\xi e^{\xi} + \frac{G}{\Pi}\{M_1[2\zeta^2 sh\zeta - \frac{(2-m)\zeta - \frac{4\zeta^3}{\Pi}}{\Pi}ch\zeta] - M_2\{\zeta e^{\zeta}[(2-m)+2\zeta - \frac{4\zeta^2}{\Pi}]\}\}$$

$$= \frac{\tau_b}{N_v}\{Ae^{-\xi} + Be^{\xi} + G\{\frac{M_1}{\Pi}[-2\zeta ch\zeta + (\frac{4\zeta^2}{\Pi} + m)sh\zeta] - M_2[\frac{m}{\xi^2} + \frac{e^{\zeta}}{\Pi}(m + \frac{4\zeta^2}{\Pi} - 2\zeta)]\}\}$$

$$\sigma = -1 \tag{26}$$

From (25) and (26), the constants A and B can be obtained:

$$A = B + M_4 \tag{27}$$

$$B = -\frac{[G\,M_3 - M_4(\xi - \frac{\tau_b}{N_v})e^{-\xi}]}{2(\xi\sinh\xi + \frac{\tau_b}{N_v}\cosh\xi)} \tag{28}$$

in which

$$M_3 = \frac{M_1}{\Pi}\{\frac{\tau_b}{N_v}(\frac{4\zeta^2}{\Pi} + m)\sinh\zeta - \frac{2\tau_b}{N_v}\zeta\cosh\zeta - 2\zeta^2\sinh\zeta - [(2-m)\zeta - \frac{4\zeta^3}{\Pi}]\cosh\zeta\}$$

$$-M_2\{\frac{m\tau_b}{\xi^2 N_v} + (m + \frac{4\zeta^2}{\Pi} - 2\zeta)\frac{\tau_b e^{\zeta}}{N_v\Pi} - [(2-m)+2\zeta - \frac{4\zeta^2}{\Pi}]\frac{\zeta\ e^{\zeta}}{\Pi}\} \tag{29}$$

and

$$M_4 = \frac{[\frac{\tau_w}{N_v} - \frac{(2-m)\zeta - \frac{4\zeta^3}{\Pi}}{\Pi}G\ (M_1 - M_2)]}{\xi} \tag{30}$$

To obtain the complete three-dimensional velocity field, the Cartesian vertical velocity, w_0, may be determined from the continuity equation. In three dimensional cylindrical coordinates, with variation in the azimuthal direction neglected and σ coordinates in vertical direction, the continuity equation is:

$$\frac{-2\sigma h}{r^2}\frac{\partial}{\partial\sigma}(ru_0) + \frac{h}{r}\frac{\partial}{\partial r}(ru_0) + \frac{\partial w_0}{\partial\sigma} = 0 \tag{31}$$

Integration of equation (31) vertically over σ from σ to 0 and

from σ to -1, and incorporation of surface boundary conditions, $w_0(r,0)=0$ (impermeability condition) and bottom boundary condition $w_0(r,-1)=-U_0\frac{\partial h}{\partial r}=-mh_0r^{m-1}U_0$, yields:

$$w_0(r,\sigma)=\int_0^{\sigma}[\frac{2\sigma h}{r^2}\frac{\partial}{\partial\sigma}(rU_0)-\frac{h}{r}\frac{\partial}{\partial r}(rU_0)]d\sigma+w_0(r,0) \tag{32}$$

and

$$w_0(r,\sigma)=\int_{-1}^{\sigma}[\frac{2\sigma h}{r^2}\frac{\partial}{\partial\sigma}(rU_0)-\frac{h}{r}\frac{\partial}{\partial r}(rU_0)]d\sigma+w_0(r,-1) \tag{33}$$

Multiplying equation (32) by (σ+1) and subtracting equation (33) multiplied by σ yields:

$$\begin{aligned}w_0(r,\sigma)&=(\sigma+1)R(r,\sigma)|_0^{\sigma}-\sigma R(r,\sigma)|_{-1}^{\sigma}+(\sigma+1)w_0(r,0)-\sigma w_0(r,-1)\\&=R(r,\sigma)-(\sigma+1)R(r,0)+\sigma R(r,-1)+(\sigma+1)w_0(r,0)-\sigma w_0(r,-1)\end{aligned} \tag{34}$$

In which $R(r,\sigma)$, $R(r,0)$, $R(r,-1)$, $w_0(r,0)$, $w_0(r,-1)$ are:

$$\begin{aligned}R(r,\sigma)&=\int[\frac{2\sigma h}{r^2}\frac{\partial}{\partial\sigma}(rU_0)-\frac{h}{r}\frac{\partial}{\partial r}(rU_0)]d\sigma\\&=hr^{m-2}\{A(2\xi\sigma-2-m)\frac{e^{\xi\sigma}}{\xi}+B(2\xi\sigma+2+m)\frac{e^{-\xi\sigma}}{\xi}+G\{\frac{M_1}{\Pi}[4\zeta^1\sigma^2+\\&\frac{4(m+2)\zeta}{\Pi}+\frac{(2+m)^2}{\zeta}]\cosh(\zeta\sigma)-(\frac{2\zeta^2}{\Pi}+1+m)\\&4\sigma\sinh\zeta\sigma]-M_2\{[\frac{4\zeta^2}{\Pi}(2+2\zeta\sigma+m)+4\zeta\sigma(1+m+\zeta\sigma)+\\&(2+m)^2]\frac{e^{-\zeta\sigma}}{\zeta\Pi}-\frac{m^2\sigma}{\xi^2}\}\}\}\end{aligned} \tag{35}$$

$$R(r,0)=hr^{m-2}(2+m)\{-\frac{A}{\xi}+\frac{B}{\xi}+G\{\frac{M_1}{\Pi}[\frac{4\zeta}{\Pi}+\frac{(2+m)}{\zeta}]-\frac{M_2}{\Pi\zeta}[(2+m)\ +\frac{4\zeta^2}{\Pi}]\}\} \tag{36}$$

$$R(r,-1) = hr^{m-2}\{-A(2\xi+2+m)\frac{e^{-\xi}}{\xi} + B(-2\xi+2+m)\frac{e^{\xi}}{\xi} + G\{\frac{M_1}{\Pi}[4\zeta +$$

$$\frac{(2+m)^2}{\zeta} + \frac{4\zeta(m+2)}{\Pi}]\cosh\zeta - 4(1+m+\frac{2\zeta^2}{\Pi})\sinh\zeta] -$$

$$M_2\{[(2+m)^2 - 4\zeta(1+m-\zeta) + \frac{4\zeta^2(2-2\zeta+m)}{\Pi}]\frac{e^{\zeta}}{\zeta\Pi} + \frac{m^2}{\xi^2}]\}\} \quad (37)$$

$$w_0(r,0) = 0 \quad (38)$$

$$w_0(r,-1) = -U_0(r,-1)\frac{\partial h}{\partial r}$$

$$= -hmr^{m-2}\{Ae^{-\xi} + Be^{\xi} + G\{\frac{M_1}{\Pi}[-2\zeta\cosh\zeta$$

$$+(\frac{4\zeta^2}{\Pi} + m)\sinh\zeta] - M_2[(m+\frac{4\zeta^2}{\Pi} - 2\zeta)\frac{e^{\zeta}}{\Pi} + \frac{m}{\xi^2}]\}\} \quad (39)$$

Test Cases

The solution presented herein incorporates several features which should be of interest to those working with numerical models. The inclusion of wind stress, baroclinic forcing, vertical mixing, bottom friction, nonlinear bottom slope, and horizontal and vertical velocity give a broad spectrum of conditions against which model features can be tested. The availability of complete solutions for velocity provides the means for verification of the computed flow field, which are in many practical cases the most important aspect of a problem. The solutions for two dimensional polar geometry are especially interesting, since they can be used to compare with three dimensional numerical model outputs in a Cartesian coordinate system.

Here, the two analytical evaluations have been given to compare with the output of a three dimensional finite element numerical model output, in order to show the utility of the analytical solutions. At the same time, they also show a sensitivity to vertical viscosity which is of considerable practical importance. The detailed description of the three dimensional finite element model, LACOM3D (Lake and Coastal Model-Three Dimensions),and extensive comparison with different analytical solutions are left to a future study.

We solve this problem on the mesh depicted in Fig. (1a), with 825 nodes and 1536 triangular elements in the horizontal and

16 evenly spaced levels in the vertical. The bottom slope, as shown in Fig. (1b), is quadratic in r such that $h = h_0 r^2$ with $h_0 = 6.25x10^{-9}/m$. At the surface the heat flux, $F_0 = 5x10^{-4}\ ^oCs^{-1}$, and wind stress, $\tau_w = -5x10^{-11}ms^{-2}$, are applied with $\omega = 7.27205x10^{-5}$ corresponding to a forcing period of 24 hours. The temperature at the bottom, $B_0 = 4\ ^oC$, and bottom friction, $\tau_b = 1x10^{-4}s^{-1}$ are specified in the examples. The unforced open boundary is applied at both the inner and outer boundaries. The temperature volume expansion coefficient, a_T, is determined by linear least squares fit of general relationship between density and temperature for fresh water, which is $-0.169695kgm^{-3}\ ^oC^{-3}$. The diffusivity coefficient $N_T = 1x10^{-5}s^{-1}$ corresponding to spin-up time around 1 day, is used during the test period. The numerical model was run from rest. The baroclinic term is computed in the σ coordinate system in LACOM3D as opposed to the z-level coordinate system, the time step is 10 seconds.

Fig.(2a) and Fig.(2b) display results for $Pr = 1$. Since the strongest wind stress and maximum heat flux at the surface are at t=0 and every 24 hours there after, and also because of the spin-up time is about 24 hours, in Fig. (2a) the comparison of currents and temperature along a radial cross section between the analytical and the numerical model outputs at t=24 hours is given. It can be seen that after 24 hours spin-up time the numerical model output matches the analytical result very well, and it also shows that the upper portion is dominated by wind and the lower is driven by the baroclinic forcing. Fig. (2b) shows that after 102 hours (the external forces are minimum), the numerical model does not show error cumulating problem, and baroclinic term controls most of water body except for the near surface part due to inertia.

The second test uses the same parameters as test one except that vertical eddy viscosity is 10 times larger than the temperature diffusivity, the result are shown in Fig.(3a) and Fig.(3b). It is obvious that not only the velocity is much weaker, but also it shows more uniform flow field due to higher viscosity. These solutions show a sensitivity to vertical viscosity which is of considerable practical importance. As a result they constitute a useful test problem.

Discussion and Conclusions

An analytical solution for baroclinic and wind forcing with internal and bottom friction and varying depth has been given for a 3D domain. The solutions differ depending on whether temperature diffusivity is equal to the vertical viscosity. All terms included in the analytical solution are important

factors for any real three dimensional numerical model, so it should be a useful tool in verifying three dimensional models and to evaluate different numerical schemes. Though the analytical solutions represent a two dimensional domain in radial coordinate system, it does not reduce its usefulness for verifying three dimensional numerical models since most models are constructed in a Cartesian coordinate system.

Although the solution presented consist of elementary transcendental functions, for ease of implementation by the coastal modelling community the authors will supply upon request a copy of the FORTRAN source code for the analytical expressions presented herein.

We advocate continual research into the development of analytical solutions for numerical model testing. An obvious advance of our solution would be to include the free surface term. Moreover, inclusion of advection and rotation would be valuable.

Reference:

Beletsky D., O'Connor W.P., Schwab D. J. and Dietrich D. E. "Numerical Simulation of Internal Kelvin Waves and Coastal Upwelling Fronts" J. Phys. Oceanogr. 21:pp. 1197-1215 1997.

Beyer H. W. "Handbook of Mathematical Sciences 6th Edition" CRC Press Inc. 1987.

Farrow D. E. and Patterson J. C. "The Daytime Circulation and Temperature Structure in a Reservoir Sidearm", Int. J. Heat Mass Transfer. Vol. 37, No. 13, pp. 1957-1968,1994.

Farrow D. E. and Patterson J. C. "On the Response of a Reservoir Sidearm to Diurnal Heating and Cooling", J. Fluid Mech. 246, pp. 143-161, 1993.

Fortunato A. B. and Baptista A. M. "Evaluation of Horizontal Gradients in Sigma-Coordinate Shallow Water Models", Atmos. Ocean 34(3) pp. 490-513 1996.

Hackett B. and Roed L. F. "Numerical Modelling of the Halton Bank Area: a Validation Study" Tellus, 46A, pp. 113-133, 1994.

Haney R. L. "On the Pressure Gradient Force over Steep Topography in Sigma Coordinate Model" J. Phys. Oceanogr. 21:pp. 610-619 1991.

Hannah C. G. and Wright D. G. "Depth Dependent Analytical and Numerical Solutions for Wind-Driven Flow in the Coastal Ocean" In Quantitative Skill Assessment for Coastal Ocean Models Eds Lynch and A. M. Davies AGU, pp. 125-152 1995.

Loder J. W. Ph.D. Thesis, Dalhousie University, 1980.

Lynch D. R. and Gray W. G., " Analytic solutions for computer flow model testing", Journal of the Hydraulics Division, ASCE, 104(HY10),pp. 1409-1428 1978.

Lynch D. R. and Officer C. B., "Analytic test cases for three-dimensional hydrodynamic models", International Journal for Numerical Methods in Fluids,5,pp. 529-543 1985.

Lynch D. R. and Werner F. E. "Three-Dimensional Hydrodynamics on Finite Element. Part I: Linearized Harmonic Model" International Journal for Numerical Methods in Fluid, Vol. 7, pp. 871-909 1987.

Maas Leo R. M. and Lam Frans-Peter A. "Geometric Focusing of Internal Waves", J. Fluid Mech. , 300,pp. 1-41,1995.

Muccino J. C., Gray W. G. and Forman M. G. "Calculation of Vertical velocity in Three-Dimensional, Shallow Water Equation, Finite Element Models", Journal for Numerical Methods in Fluids,25,pp. 779-802 1997.

Tartinville B., Deleersnijder E., Lazure P., Proctor R., Ruddick K. G., and Uittenbogaard R. E. "A Coastal Ocean Model Intercomparison Study for a Three-dimensional Idealised Test Case" Applied Mathematical Modelling 22 pp. 165-182 1998.

List of Figure Captions

1a) Plan view of the quarter annulus with inner and outer boundaries.

1b) Cross sectional view of the quarter annulus with quadratic bottom dependence.

2a) Comparison of currents and temperature along a radial cross section between the analytical and the numerical model outputs for viscosity equal to temperature diffusivity after 24 hours (as external forces are maximum).

2b) The same comparison as Fig.(2a) after 102 hours (as external forces are minimum).

3a) The same comparison as Fig.(2a) except for a viscosity 10 times larger than the temperature diffusivity.

3b) The same comparison as Fig.(3a) after 102 hours.

Appendix A: Details of the Particular Solutions

For ease of presentation , we rewrite equation (17) as:

$$\frac{\partial^2 u_0}{\partial \sigma^2} - \xi^2 u_0 = \frac{a_T g h_0}{\rho_w \zeta N_v}\{M_2[m-(m+2\sigma\zeta)e^{-\zeta\sigma}] + M_1[2\sigma\zeta\cosh(\zeta\sigma) - m\sinh(\zeta\sigma)]\} \qquad (A1)$$

The right hand side can be rearranged in exponential function form as:

$$RH = \frac{a_T g h_0}{\rho_w \zeta N_v}\{mM_2 - \frac{mM_1}{2}e^{\zeta\sigma} + m(\frac{M_1}{2} - M_2)e^{-\zeta\sigma} + M_1\zeta\sigma e^{\zeta\sigma} + (M_1 - 2M_2)\zeta\sigma e^{-\zeta\sigma}]\} \qquad (A2)$$

The expression (A2) can be classified as three different forms which are:

$$RH1 = 1 \qquad (A3)$$

$$RH2 = e^{\pm\zeta\sigma} \qquad (A4)$$

$$RH3 = \sigma e^{\pm\zeta\sigma} \qquad (A5)$$

The left hand side of (A1) can be written as:

$$LH = (D^2 - \xi^2)u_0 = f(D)u_0 \qquad (A6)$$

Where $D = \frac{\partial}{\partial\sigma}$ and $D^2 = \frac{\partial^2}{\partial\sigma^2}$. The solution for RH1 term is:

$$u_1 = -\frac{1}{\xi^2} \qquad (A7)$$

In order to solve RH2 term the following formulas (Beyer H. W.,1987) have to be used depending on weather $\xi \neq \zeta$ or $\xi = \zeta$. For the $\xi \neq \zeta$ case,

$$\frac{1}{f(D)}e^{ax} = \frac{1}{f(a)}e^{ax} \qquad (A8)$$

therefore,

$$u_2 = \frac{1}{D^2 - \xi^2}e^{\pm\zeta\sigma} = \frac{1}{\zeta^2 - \xi^2}e^{\pm\zeta\sigma} \qquad (A9)$$

For the $\xi=\zeta$ case, due to $\zeta^2-\xi^2=0$, the formula (A7) is unsuitable. In this case

$$\frac{1}{f(D)}e^{ax} = \frac{x}{f'(a)}e^{ax} \tag{A10}$$

has to be used. So

$$u_2 = \frac{1}{D^2-\xi^2}e^{\pm\zeta\sigma} = \pm\frac{\sigma}{2\zeta}e^{\pm\zeta\sigma} \tag{A11}$$

By applying the formula (Beyer H. W.,1987)

$$\frac{1}{f(D)}e^{ax}V(x) = e^{ax}\frac{1}{f(D+a)}V(x) \tag{A12}$$

the RH3 term can be solved as:

$$\begin{aligned} u_3 &= \frac{1}{D^2-\xi^2}\sigma e^{\pm\zeta\sigma} \\ &= e^{\pm\zeta\sigma}\frac{1}{(D\pm\zeta)^2-\xi^2}\sigma \\ &= e^{\pm\zeta\sigma}\frac{1}{D^2\pm 2D\zeta+\zeta^2-\xi^2}\sigma \end{aligned} \tag{A13}$$

In order to solve u_3, the conditions for $\xi\neq\zeta$ with $\xi=\zeta$ have to be considered separately. For case $\xi\neq\zeta$, let:

$$\frac{1}{D^2\pm 2D\zeta+\zeta^2-\xi^2} = c_0 + c_1 D + R(D^2) \tag{A14}$$

$R(D^2)$ represents the D terms of higher than the first power. Multiplying two sides of (A14) by $D^2\pm 2D\zeta+\zeta^2-\xi^2$ and only keeping the D terms of less than second power, the constants c_0 and c_1 can be computed by comparing the terms of the same power in D on the two sides of (A15),

$$1 = c_0(\zeta^2-\xi^2)\pm c_0\zeta 2D + c_1(\zeta^2-\xi^2)D \tag{A15}$$

$$c_0 = \frac{1}{\zeta^2-\xi^2} \tag{A16}$$

$$\pm c_0 2\zeta + c_1(\zeta^2-\xi^2) = 0 \tag{A17}$$

$$c_1 = \mp\frac{2\zeta}{(\zeta^2-\xi^2)^2} \tag{A18}$$

So u_3 can be obtained as

$$u_3 = e^{\pm\zeta\sigma}\frac{1}{D^2 \pm 2D\zeta + \zeta^2 - \xi^2}\sigma$$
$$= e^{\pm\zeta\sigma}\left(\frac{1}{(\zeta^2-\xi^2)} \mp \frac{2\zeta}{(\zeta^2-\xi^2)^2}\frac{\partial}{\partial\sigma}\right)\sigma$$
$$= e^{\pm\zeta\sigma}\left(\frac{\sigma}{(\zeta^2-\xi^2)} \mp \frac{2\zeta}{(\zeta^2-\xi^2)^2}\right) \qquad (A19)$$

When $\xi=\zeta$, the above method is unable to resolve c_0 and c_1. However, by rearranging f(D) (A13) as:

$$f(D) = D^2 \pm 2D\zeta = D(D \pm 2\zeta) = Dh(D) \qquad (A20)$$

and applying the following formula:

$$\frac{1}{f(D)}V(x) = \frac{1}{D^k}\frac{1}{h(D)}V(x) = \underbrace{\int\cdots\int}_{k}\frac{1}{h(D)}V(x)(dx)^k \qquad (A21)$$

and as before, expanding $\frac{1}{D\pm 2\zeta}$ as a polynomial of D:

the solution (A13) become:

$$u_3 = e^{\pm\zeta\sigma}\frac{1}{D^2 \pm 2D\zeta}\sigma$$
$$= e^{\pm\zeta\sigma}\frac{1}{D(D \pm 2\zeta)}\sigma$$
$$= e^{\pm\zeta\sigma}\int\frac{1}{(D \pm 2\zeta)}\sigma\, d\sigma$$
$$= e^{\pm\zeta\sigma}\int\frac{1}{2\zeta}\left(\pm 1 - \frac{1}{2\zeta^2}\frac{\partial}{\partial\sigma}\right)\sigma\, d\sigma$$
$$= \frac{e^{\pm\zeta\sigma}\sigma}{4\zeta}\left(\pm\sigma - \frac{1}{\zeta}\right) \qquad (A22)$$

Combining solutions for RH1, RH2 and RH3 with corresponding factors, the particular solution for equation (A1) can be obtained. When $\xi \neq \zeta$

$$Q_{\xi\neq\zeta} = \frac{g a_T h_0}{\rho_w \zeta N_v}\left[-\frac{mM_2}{\xi^2} - \frac{mM_1 e^{\zeta\sigma}}{2(\zeta^2-\xi^2)} + m\left(\frac{M_1}{2} - M_2\right)\frac{e^{-\zeta\sigma}}{\zeta^2-\xi^2} + \left(\sigma - \frac{2\zeta}{\zeta^2-\xi^2}\right)\frac{\zeta M_1 e^{\zeta\sigma}}{\zeta^2-\xi^2}\right.$$
$$\left. + (M_1 - 2M_2)\left(\sigma + \frac{2\zeta}{\zeta^2-\xi^2}\right)\frac{\zeta e^{-\zeta\sigma}}{\zeta^2-\xi^2}\right.$$

$$= \frac{ga_T h_0}{\rho_w \zeta N_\nu}\{\frac{M_1}{\zeta^2-\xi^2}[2\zeta\sigma\cosh(\zeta\sigma) - (\frac{4\zeta^2}{\xi^2-\xi^2}+m)\sinh(\zeta\sigma)] -$$

$$M_2[\frac{m}{\xi^2} + \frac{e^{-\zeta\sigma}}{\zeta^2-\xi^2}(2\zeta\sigma + \frac{4\zeta^2}{\zeta^2-\xi^2}+m)]\} \qquad (A23)$$

and for $\xi = \zeta$

$$Q_{\xi=\zeta} = \frac{ga_T h_0}{\rho_w \zeta N_\nu}[-\frac{mM_2}{\zeta^2} - \frac{mM_1\sigma e^{\zeta\sigma}}{4\zeta} - m(\frac{M_1}{2}-M_2)\frac{\sigma e^{-\zeta\sigma}}{2\zeta} + \frac{M_1}{4}(\sigma - \frac{1}{\zeta})e^{\zeta\sigma} -$$

$$(M_1 - 2M_2)(\sigma + \frac{1}{\zeta})\frac{\sigma e^{-\zeta\sigma}}{4}]$$

$$= \frac{ga_T h_0}{2\rho_w \zeta^2 N_\nu}\{M_2[(m+1+\zeta\sigma)\sigma e^{-\zeta\sigma} - \frac{2m}{\zeta}] +$$

$$M_1\sigma[\zeta\sigma\sinh(\zeta\sigma) - (m+1)\cosh(\zeta\sigma)]\} \qquad (A24)$$

Appendix B: Vertical Velocity for Case $\xi = \zeta$

Due to the fact that the particular solution to equation (17) is different for the cases $\xi = \zeta$ and $\xi \neq \zeta$, the constants A and B in solution (20) and the solution for the vertical velocity will be different in the two different cases. Here, the final results for the case $\xi = \zeta$ are given, which can be obtained by a similar method in the case $\xi \neq \zeta$ as mentioned before

$$A = B + M_4 \qquad (B1)$$

$$B = \frac{[GM_3 + e^{-\xi}(\xi - \frac{\tau_b}{N_\nu})M_4]}{2(\xi\ \sinh\xi + \frac{\tau_b}{N_\nu}\cosh\xi)} \qquad (B2)$$

$$M_4 = \frac{\frac{\tau_w}{N_\nu} - G(m+1)(M_2 - M_1)}{\xi} \qquad (B3)$$

$$G = \frac{ga_T h_0}{2\rho_w \xi^2 N_\nu} \qquad (B4)$$

$$M_3 = M_2\{[(m+1) - \xi(1-m) - \xi^2 + \frac{(m+1-\zeta)\tau_b}{N_\nu}]e^\xi + \frac{2m\tau_b}{N_\nu\xi}\} + M_1\{[\xi^2 - (m+1) -$$

$$\frac{(m+1)\tau_b}{N_\nu}]\cosh\xi + [\frac{\zeta\tau_b}{N_\nu} - (m-1)\zeta]\sinh\xi\} \qquad (B5)$$

$$w_0(r,\sigma) = (\sigma+1)R(r,\sigma)|_0^{\sigma} - \sigma R(r,\sigma)|_{-1}^{\sigma} + (\sigma+1)w_0(r,0) - \sigma w_0(r,-1)$$
$$= R(r,\sigma) - (\sigma+1)R(r,0) + \sigma R(r,-1) + (\sigma+1)w_0(r,0) - \sigma w_0(r,-1) \qquad (B6)$$

$$R(r,\sigma) = \int [\frac{2\sigma h}{r^2}\frac{\partial}{\partial\sigma}(rU_0) - \frac{h}{r}\frac{\partial}{\partial r}(rU_0)]d\sigma$$

$$= hr^{m-2}\{A(2\xi\sigma - 2 - m)\frac{e^{\xi\sigma}}{\xi} + B(2\xi\sigma + 2 + m)\frac{e^{-\xi\sigma}}{\xi} + G\{M_2\{[\frac{(\sigma+\frac{1}{\xi})(m+2)(m+3)}{\xi} +$$

$$\sigma^2(4+3m+2\xi\sigma)]e^{-p\sigma} + \frac{2m^2\sigma}{\xi}\} + M_1\{\frac{\sigma}{\xi}[(m+2)(m+3) + 2\xi^2\sigma^2]\sinh(\xi\sigma) -$$

$$\frac{1}{\xi^2}[(4+3m)\xi^2\sigma^2 + (m+2)(m+3)]\cosh(\xi\sigma)\}\}\} \qquad (B7)$$

$$R(r,0) = hr^{m-2}[\frac{(2+m)}{\xi}(B-A) + \frac{G(m+2)(m+3)}{\xi^2}(M_2 - M_1)] \qquad (B8)$$

$$R(r,-1) = hr^{m-2}\{-A(2\xi+2+m)\frac{e^{-\xi}}{\xi} + B(-2\xi+2+m)\frac{e^{\xi}}{\xi} + G\{M_2\{[(4+3m-2\xi)$$

$$+\frac{(\frac{1}{\xi}-1)(m+2)(m+3)}{\xi}]e^{\xi} - \frac{2m^2}{\xi}] + M_1\{\frac{1}{\xi}[(m+2)(m+3) + 2\xi^2]\sinh\xi - \frac{1}{\xi^2}[(4+3m)\xi^2$$

$$+(m+2)(m+3)]\cosh\xi\}\}\} \qquad (B9)$$

$$w_0(r,0) = 0 \qquad (B10)$$

$$w_0(r,-1) = mr^{2(m-1)}h_0\{Ae^{-\xi} + Be^{\xi} + G\{M_2[(\xi-m-1)e^{\xi} - \frac{2m}{\xi}] +$$

$$M_1[(m+1)\cosh\xi - \xi\sinh\xi]\}\} \qquad (B11)$$

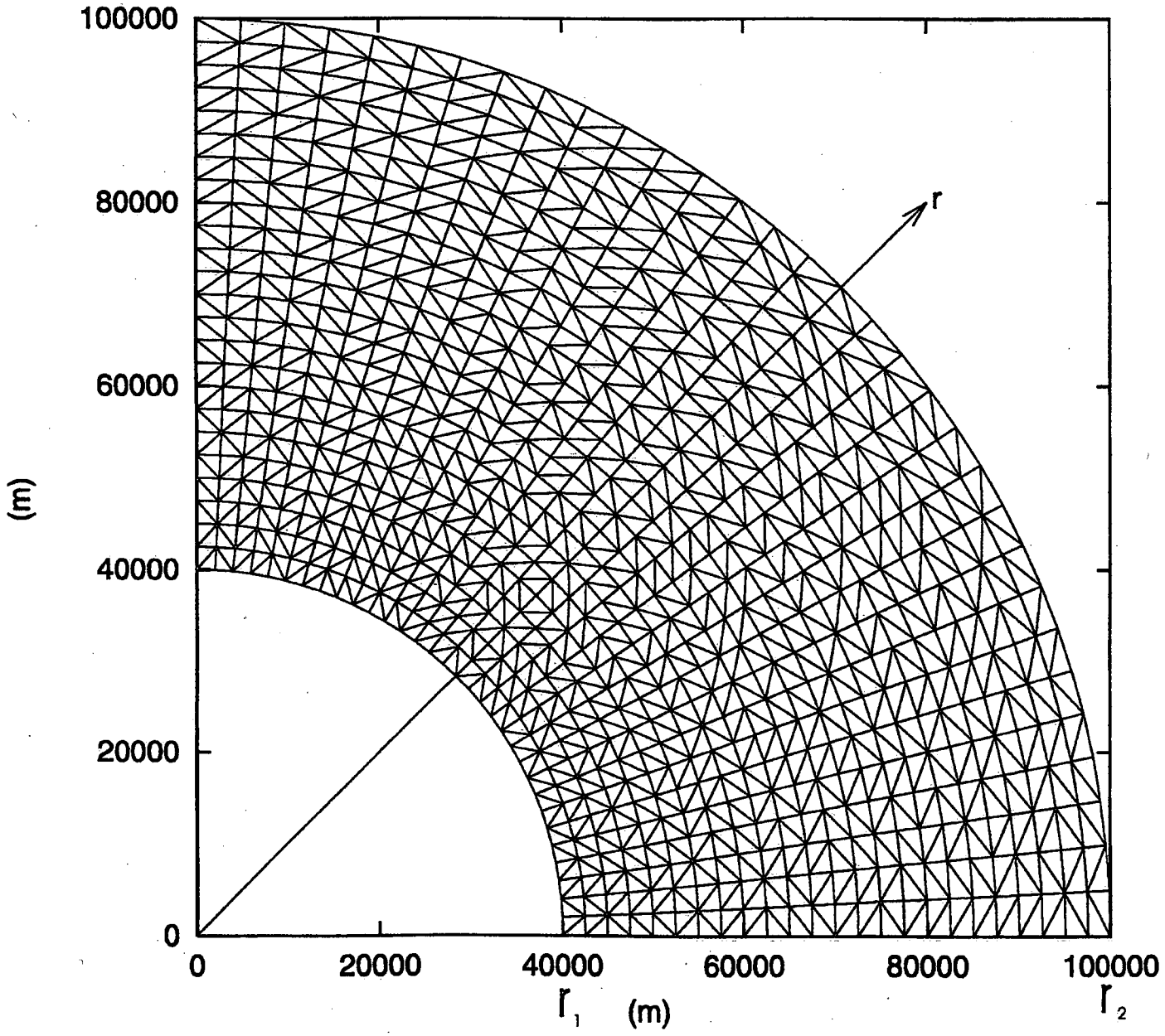
100000
80000
60000
40000
20000
0
(m)
r
0
20000
40000
60000
80000
100000
r1 (m)
r2

Fig. (1a)

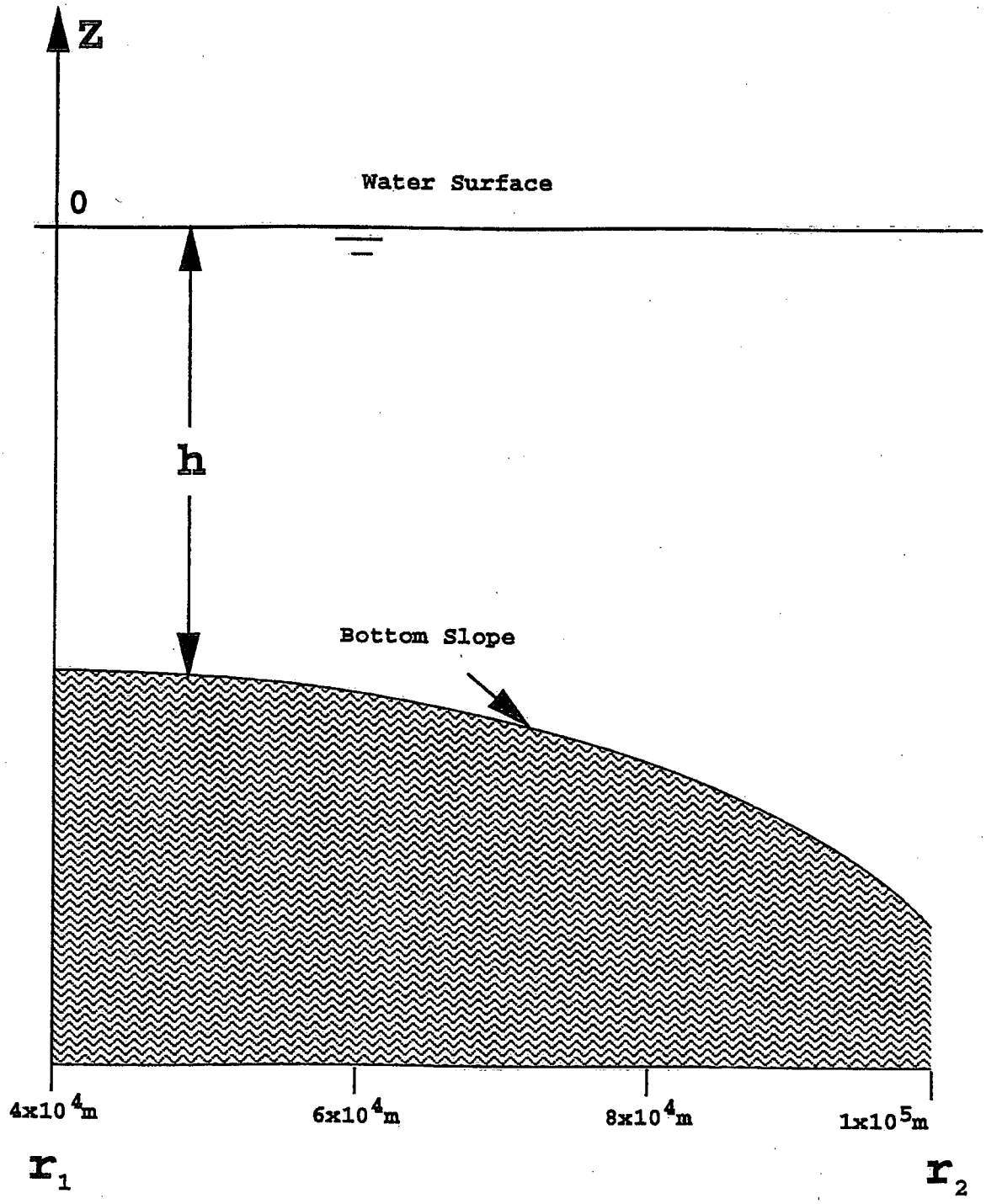
z
0
Water Surface
h
Bottom Slope
4x10 4m
6x10 4m
8x10 4m
1x10 5m
r1
r2

Fig. (16)

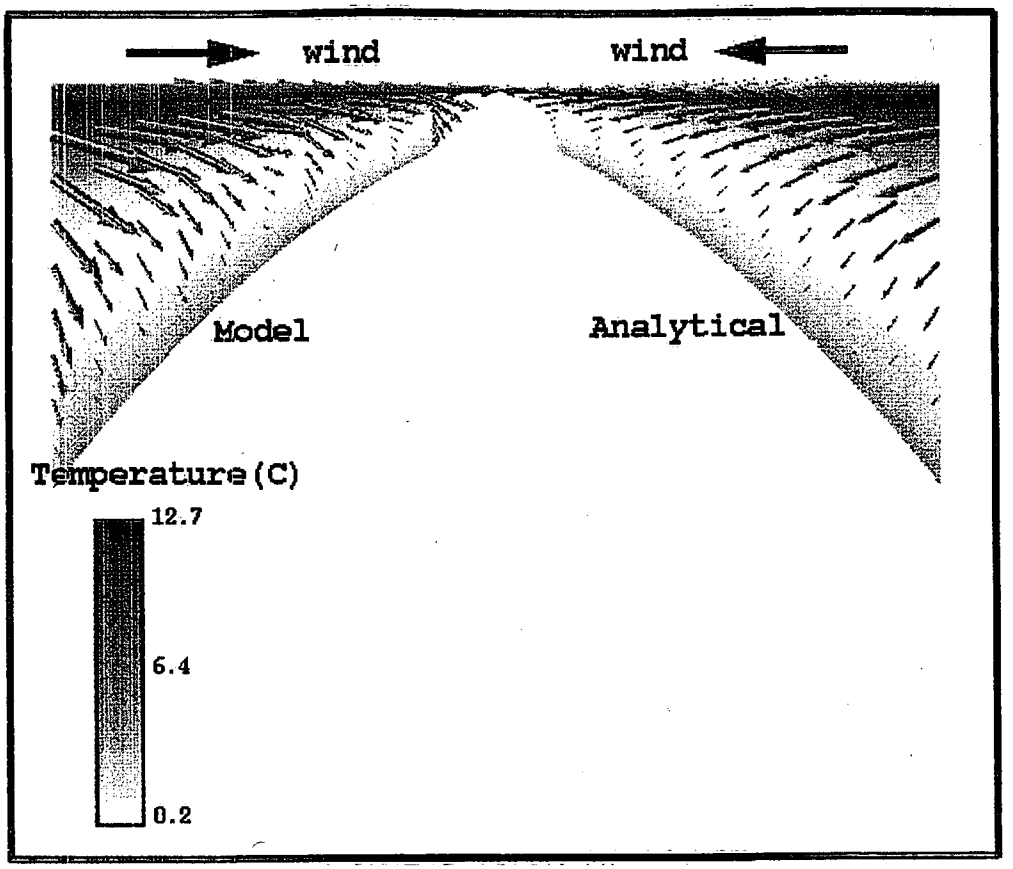

Fig. (2a)

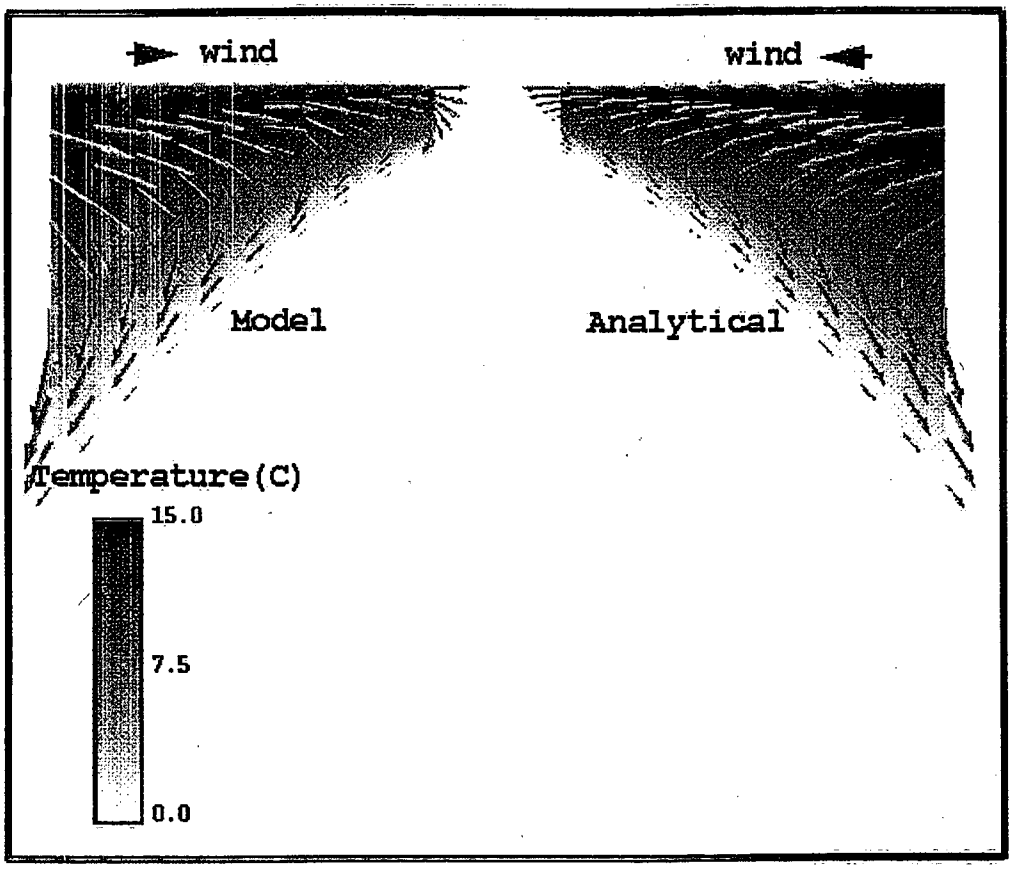

Fig. (2b)

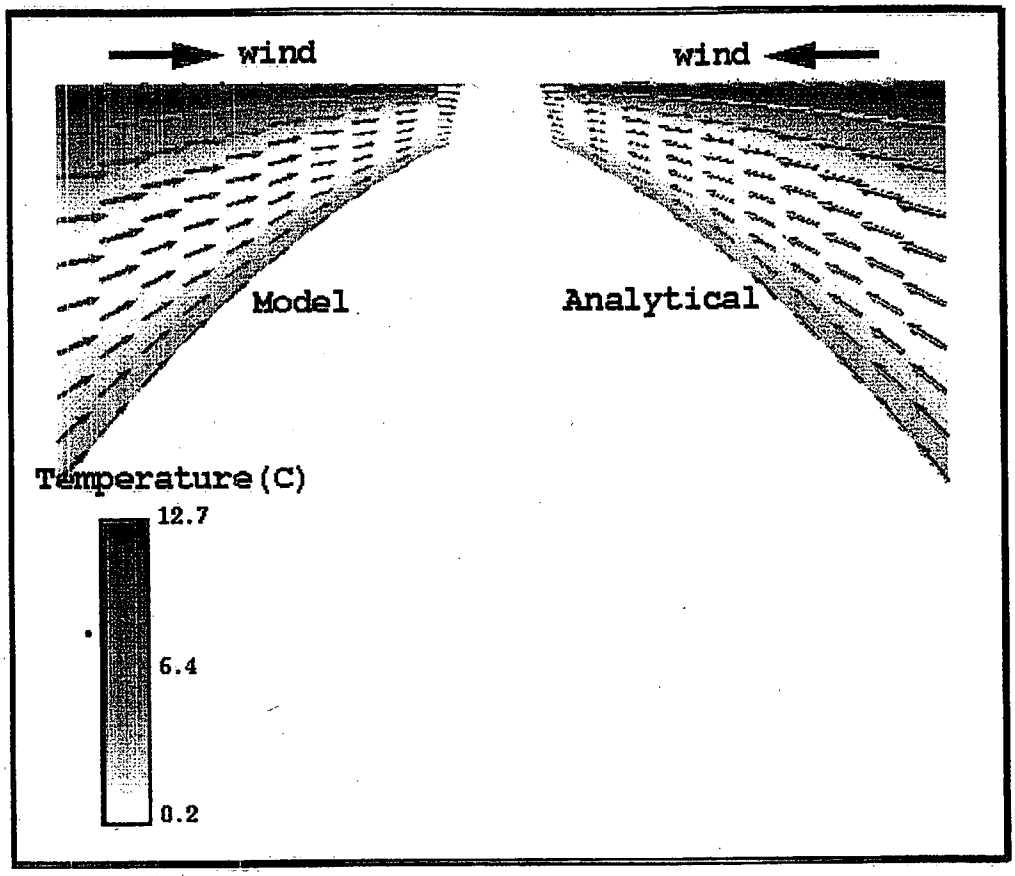

Fig (3a)

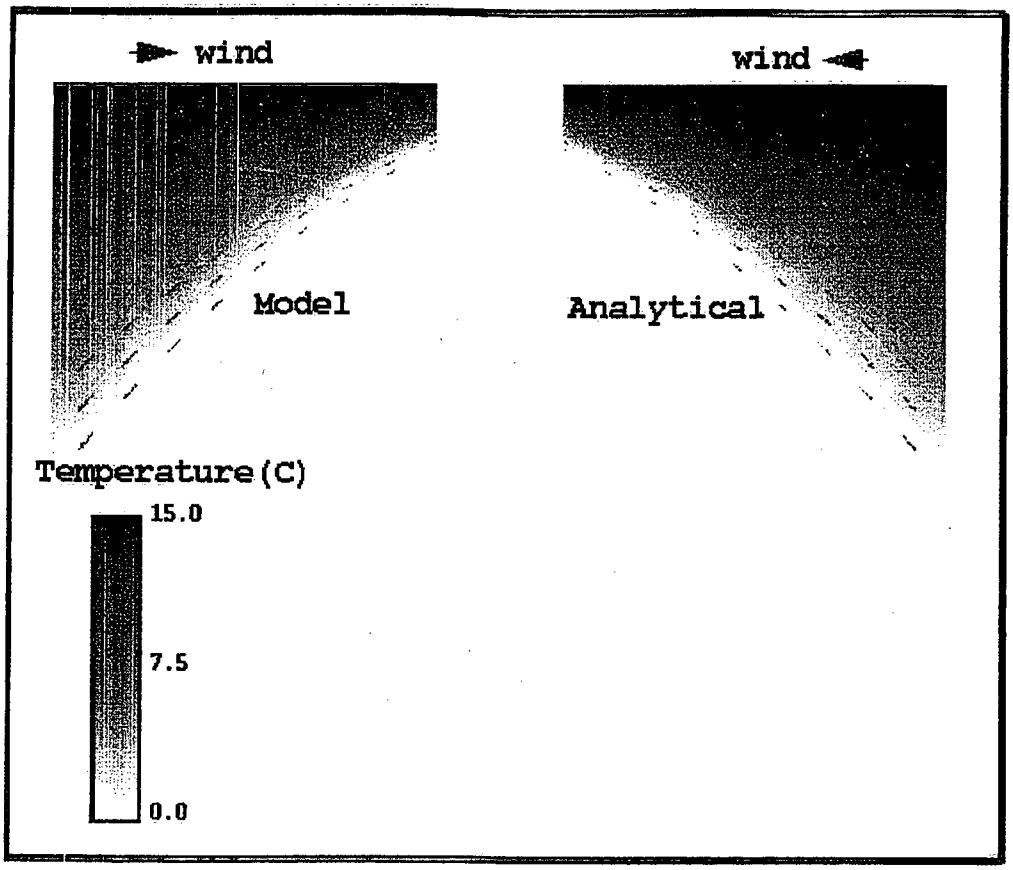

Fig. (3b)

Environment Canada Environnement Canada

Canada

Canada Centre for Inland Waters
P.O. Box 5050
867 Lakeshore Road
Burlington, Ontario
L7R 4A6 Canada

National Hydrology Research Centre
11 Innovation Boulevard
Saskatoon, Saskatchewan
S7N 3H5 Canada

St. Lawrence Centre
105 McGill Street
Montreal, Quebec
H2Y 2E7 Canada

Place Vincent Massey
351 St. Joseph Boulevard
Gatineau, Quebec
K1A 0H3 Canada

Centre canadien des eaux intérieures
Case postale 5050
867, chemin Lakeshore
Burlington (Ontario)
L7R 4A6 Canada

Centre national de recherche en hydrologie
11, boul. Innovation
Saskatoon (Saskatchewan)
S7N 3H5 Canada

Centre Saint-Laurent
105, rue McGill
Montréal (Québec)
H2Y 2E7 Canada

Place Vincent-Massey
351 boul. St-Joseph
Gatineau (Québec)
K1A 0H3 Canada